Research Article ISSN 2833-0390

International Journal of Research in Oncology

New Regulatory roles for Human Serum Amyloid A

Carlos G. García-Cortés and Elsie I. Parés-Matos*

Department of Chemistry, University of Puerto Rico at Mayagüez, CALL BOX 9000, Mayagüez, PR 00681-9000

***Correspondence:**
Elsie I. Parés-Matos, Department of Chemistry, University of Puerto Rico at Mayagüez, CALL BOX 9000, Mayagüez, PR 00681-9000.

Received: 02 Mar 2024; **Accepted:** 07 Apr 2024; **Published:** 13 Apr 2024

Citation: García-Cortés CG, Parés-Matos EI. New Regulatory roles for Human Serum Amyloid A. Int J Res Oncol. 2024, 3(1): 1-8.

ABSTRACT

The current study illuminates the multifaceted role of Serum Amyloid A (SAA), an essential acute-phase protein implicated in diverse biological realms, encompassing inflammation, oncogenesis, and stress modulation. With a focus on delineating the intricate protein-protein interactions orchestrated by SAA, this investigation unravels its diverse functions within the human physiological landscape. Utilizing the HepG2 cell line, renowned for its proficiency in facilitating SAA overexpression, we meticulously generated protein extracts after inducing SAA hyperexpression. Integrating Co-Immunoprecipitation techniques with Liquid Chromatography-Tandem Mass Spectrometry (LC/MS/MS) enabled discernment and characterization of the protein complexes intricately associated with SAA. Our data elucidates a pronounced upregulation in SAA expression levels within induced samples compared to controls, substantiating its pivotal role among inflammatory cascades. Specifically, LC/MS/MS profiling delineated interactions with nine distinct proteins, encompassing pivotal players in actin dynamics, neuronal morphogenesis, lipid homeostasis, and immunomodulation. Furthermore, this investigation underscores the plausible ramifications of these molecular interactions in pathologies, including Alzheimer's disease, oncological manifestations, and rheumatoid arthritis. Through comprehensive analyses, this investigation sheds light on the intricate roles of SAA and provides a foundation for future therapeutic modalities targeting SAA pathologies.

Keywords

Acute-Phase Response, Co-Immunoprecipitation, Mass Spectrometry, Serum Amyloid A.

Introduction

Homeostasis is a variety of processes by which biological systems tend to maintain stability. Many biological pathways or processes exist to support this state. Among them is the Acute Phase Response (APR). The APR comprises a categorized arrangement of anatomical responses – fever, hormonal changes, metabolic alterations due to inflammation, cancer, trauma, stress, and other events [1]. Adjustment of protein concentration in human serum during APR is particularly distinctive. Serum Amyloid A (SAA) is a secreted protein prominent in APR.

The SAA protein family comprises highly conserved acute-phase proteins found in humans, cows, dogs, hamsters, mice, mink, horses, rabbits, and sheep, among other vertebrate species. SAA is an apolipoprotein synthesized primarily by the liver, but it can also be synthesized in macrophages, kidneys, testis, prostate, lung, adipocytes, and synovial cells. It is also found in the brain and mammary glands [2-6]. Early studies have revealed that four genes located in human chromosome 11p15.1 encode SAA. SAA1 and SAA2 gene products induce acute-phase reactions due to overexpression. The SAA3 gene cannot be expressed at all since this gene is a pseudogene. However, an mRNA was found to code for a predicted 42 amino acid polypeptide [3]. Meanwhile, the SAA4 gene encodes for a constitutive type of SAA, suggesting it is continuously expressed at low concentration levels [7].

In contrast, plasma levels of SAA1 and SAA2 can increase dramatically by as much as 1000-fold, reaching serum concentrations of up to 1–2 mg/ml [8]. This hyperexpression is upregulated by pro-inflammatory mediators, particularly interleukin-6 (IL-6), interleukin-1 (IL-1), tumor necrosis factor-alpha (TNF-α), interferon-γ, and transforming growth factor (TGF) [9]. Notably, persistent hyperexpression of these two isoforms causes amyloid fibrils in the reactive amyloid A amyloidosis [10]. Amyloidosis is

a clinical manifestation of patients with inflammatory problems, characterized by extracellular tissue deposition of around 76 amino acid hydrophobic fragments. These fragments come primordially from the degradation via endosomes or lysosomes of SAA1.1 after prolonged expression. Finally, it has been observed that matrix metalloproteinases (MMPs) [11] and lysosomal proteases CathB [12] cleave SAA. However, more research is needed to demonstrate whether these two macromolecules are the primary cause of amyloidosis.

The high conservation of SAA among vertebrates suggests its essential biological role. SAA is known to play a role in cholesterol and HDL metabolism. Meanwhile, it has been reported that SAA may induce cytokine, chemokine, and MMPs' expression among MMPs' cellular migration [13]. It is also linked to many inflammatory diseases like rheumatoid arthritis and chronic inflammatory bowel disease. Moreover, acute-phase SAA proteins are mainly associated with plasma high-density lipoproteins, suggesting a possible role in developing atherosclerosis [14]. The extrahepatic expression of this protein has been linked to various diseases, such as Alzheimer's disease, diabetes, cancer, and metabolic syndrome, among others [9]. High SAA concentrations in blood have been correlated with severe symptoms or death in patients with COVID-19 [15]. Recently, SAA1 has been found in human colostrum, presumably contributing to neonatal protection [3]. Even though the SAA family is linked to different diseases, little of its potential interactions with other proteins are specific or completely understood.

This research focuses on determining these protein-protein complexes with SAA to understand what other functions SAA can play in the human body. Since human SAA is primarily synthesized by liver cells, the HepG2 cell line is the best choice for SAA overexpression. HepG2 cells were isolated from a fifteen-year-old white male Caucasian who suffered from a hepatocarcinoma. These cells are known for their capability to overexpress plasma proteins, SAA among them [8]. Crude protein extracts were prepared once overexpression of SAA was achieved in HepG2 cells to obtain these protein-protein complexes. Human SAA levels were measured using an ELISA kit. Subsequently, protein complexes with human SAA were isolated through Co-Immunoprecipitation and characterized with LC/MS/MS. Finally, those protein complexes bound to SAA were analyzed according to function and cell location.

Materials and Methods

Cell culture and induction

HepG2 cells were cultured at 37°C and 5% CO_2 in 100 nm x 20 nm plates containing MEM (GIBCO 11095-080), supplemented with 10% FBS (ATCC 30-2020), and 50 U/ml penicillin and 50 µg /ml streptomycin (GIBCO; 15140-122) as described by Donato and colleagues [16]. The complete medium was changed every three days, and the cell viability was verified each time a subculturing was made. After reaching a 70% confluence, the medium was discarded, and the HepG2 cells were washed with 5 ml of fresh medium without serum. The wash was discarded and HepG2 cells were incubated for 1 h with 10 ml of fresh medium without serum. Then, for SAA hyperexpression, 100 ng/ml IL-1β (SIGMA-ALDRICH; SRP3083), 100 ng/ml IL-6 (SIGMA-ALDRICH; H7416), and 100 ng/ml Retinol (SIGMA-ALDRICH; 95144) were added as well as 100 ng/ml LPS (CALBIOCHEM; 437627) [17,18]. Subsequently, cells were incubated for 6 h and 12 h. The same amount of ethanol and water mixture was used in those culture plates used as controls.

Preparation and Quantification of Cytoplasmic Extracts

Cells were gently detached from plates with a sterile and disposable spatula, and then transferred to a 50-ml conical centrifuge tube. Subsequently, cell suspensions were spun at 5,000 rpm for 5 min at 4°C. Each supernatant was transferred to a clean 50-ml tube, and then concentrated to 1 ml in 1x PBS using a 3 kDa Amicon filter (Millipore UFC900308). Protein inhibitors (2 µg/ml leupeptin, 0.03 TiU/ml aprotinin, 1 µg/ml pepstatin, 1 mM PMSF) were added to the concentrated supernatants before its storage at -80°C. Cell pellets were resuspended in 1 ml of ice-cold 1x PBS (twice) and centrifuged for 1 min at 16,000 rpm at room temperature. HepG2 cell pellets were also stored at -80°C until their use.

Each pellet of frozen HepG2 cells was slowly defrosted by placing it on a bucket with ice before preparing cytoplasmic extracts, according to Parés-Matos PhD Thesis (2000) [19]. Then, cells were resuspended in 500 µl of ice-cold 10 mM HEPES, pH 7.9 (10 mM KCl; 0.5 mM EDTA and 0.5 mM EGTA, pH 8.0) containing 2 µg/ ml leupeptin, 0.03 TiU/ml aprotinin, 1 µg/ml pepstatin, and 1 mM PMSF (added last). The cells were allowed to swell on ice for 20 min, after which 25.0 µl of a 10% Nonidet NP-40 solution was added, and the tube was vigorously vortexed for 10 s. The homogenate was centrifuged at top speed (16,000 rpm) for 30 min at 4°C. The supernatants containing cytoplasm and RNA were frozen in aliquots (200 µl each) at -80°C or used to perform QUBIT (for determining total protein concentration assay) or ELISA (for determining SAA concentration).

Total protein concentration was calculated with a Qubit 3.0 Fluorometer (Life Technologies, Carlsbad, California, USA). Each sample was diluted with a working solution at a 1:200 ratio and analyzed in duplicate. SAA quantification was performed with a Human SAA-ELISA kit following manufacturers' instructions (SIGMA-ALDRICH; RAB0420-1KT). Samples from concentrated supernatants and crude lysates (either from uninduced or induced HepG2 cells) were diluted at a 1:2 ratio with lysis buffer, without NP-40 or proteases, in each well before ELISA analysis. Two wells for each sample were used, and 10 runs were performed for the plate using a microplate reader (450 nm). Results were normalized using lysis buffer and total protein concentration. The microplate reader used for quantified SAA was a Biotek ELx800 with the software Gen 5 version 1.11.

SDS-PAGE and Western blot

An aliquot containing 20 µg of total protein in sample buffer (Laemmli buffer with 5% of β-mercaptoethanol) was loaded onto 4%–20% TGX gels (Bio-Rad; 456- 1094) and electrophoresed

at 150 voltz for 55 min. Gels were stained overnight on a slow rocking platform with Coomassie Brilliant Blue, and then distained with two solutions: solution #1 (25% methanol + 10% acetic acid in HPLC ultrapure water) for 30 min and solution #2 (25% methanol in water) until bands were observed. PVDF membranes were probed with mouse Anti-SAA IgG [115] (1:1,000; Gene Tex GTX20687) and incubated overnight at 4°C. HRP-conjugated anti-mouse secondary antibody (1:10,000; Promega W402B) was incubated for 1 h. Images were acquired and analyzed using ImageLab software (Bio-Rad). SAA protein bands are located approximately at 12 kDa. Both essays were performed to verify the protein quality in the samples and the antibody-SAA coupling efficiency.

Isolation of Protein Complexes with SAA by Co-Immunoprecipitation

A normalized amount of 570 µg of total protein was first incubated overnight with 5 µg of mouse anti-SAA IgG [115], then bonded with the complex Pierce Protein A/G magnetic beads (REF: 90409), washed several times and eluted. Samples were suspended in 6 M Urea/50 mM TEAB, reduced with TCEP to a final concentration of 5 mM, and alkylated with iodoacetamide to a final concentration of 24 mM. Urea concentration was reduced to <1M, and proteins were digested with Trypsin overnight. The next day, samples were acidified with 10% TFA, centrifuged to recover supernatant, and dried in a speed vacuum. Thereafter, samples were desalted following the instructions specified for the Pierce C18 Spin Columns (REF: 89870). Cleaned peptides eluted from the spin columns were dried in a speed vacuum and stored at -20°C until mass spectrometry analysis. Negative control was prepared by performing immunoprecipitation with magnetic beads without antibodies.

LC-MS/MS Analysis

A PicoChip H354 REPROSIL-Pur C18-AQ 3 µm 120 A (75 µm x 105 mm) chromatographic column (New Objective) was used for peptide separation. The separation was obtained using a gradient of 5%-40% of 0.1% formic acid in 80% acetonitrile (Buffer B) for 45 min, 40%-95% of Buffer B for 6 min, down for 95%-5% for 6 min, 5%-95% Buffer B for 6 more min, and 95%-5% for the last 6 min. The overall total gradient was 69 min. The flow rate was set at 300 nl/min with a maximum pressure of 300 bar, and the injection volume was 2.0 µL per sample. Q-Exactive Plus operates in positive polarity mode and data-dependent mode. The full scan (MS1) was measured over the range of 400 to 1600. The MS2 (MS/MS) analysis was configured to select the ten (10) most intense ions (Top 10) for HCD fragmentation. A dynamic exclusion parameter was set for 15 s. Mass spectrometric raw data were analyzed using Proteome Discoverer (PD) software, version 2.5. Files were searched against a Human database downloaded using the PD Protein Center tool (tax ID = 9606). The only modification included was a static carbamidomethyl modification of +57.021 Da (C). Moreover, a filter was applied to only show proteins with two or more unique peptides identified. Keratins and ribosomal proteins were not considered, as they are regular contaminants or possible false positives in mass spectrometers [20]. Samples were run in duplicates, and proteins not detected in at least two equal samples were removed, which could also be a false positive result.

Computational Predictions of Complexes' Physical Interactions

Once the bound proteins were characterized, their three-dimensional structure was obtained from the Protein Data Bank (PDB) or AlphaFold (AF) data bank. The three parameters used for choosing each structure were (a) human, (b) completed sequence without a signal peptide, and (c) no mutations. If none of these parameters were found in the PDB's experimental crystallography structure, then a predicted AF model was chosen. Once the chosen structures were cleaned (necessary to remove ions, water, or organic molecules), all .pdb files were submitted to the ClusPro server (http://nrc.bu.edu/cluster) for protein-protein docking. After the ClusPro run finished, the complex file with the lowest energy, usually described or ranked as complex #0 in balance-type interactions, was downloaded, and submitted to PDBsum. Then, the files were analyzed by the PDBsum server, given the number of H-bonds, salt bridges, non-bonded interactions, and the number of residues of each protein interacting in each complex. Finally, the PDBsum files were analyzed and contrasted with each other to determine the most reactive residues of SAA.

Results and Discussion

As shown in Figure 1A, there is no significant difference in the total cytoplasmic protein levels between the control group and the cytoplasmic protein-induced samples. However, a notable observation was that the total cytoplasmic protein induced for 12 h and 6 h showed slightly more protein than their controls. In contrast, statistical analysis of the data revealed a significant decrease in the total protein secretion levels in the induced samples compared to the controls. These findings agree with previous studies, which have demonstrated a reduction in total protein secretion after cells are treated with IL-1B, IL-6, LPS, and Retinol, despite the general belief that such treatments increase protein production and secretion [21,22]. Moreover, a statistical difference was observed between secreted-induced samples incubated for 6 h and 12 h. However, ELISA results (Figure 1B) demonstrated a high statistical difference between induced samples and controls. Samples induced for 6 h have 9x more SAA than their controls, in cytoplasmic quantification, and 6x more than controls, in secreted quantification. SAA concentration was 9x higher in 12 h cytoplasmic-induced samples and 11x higher in secreted quantification. Moreover, the results indicate a statistical difference between 12 h and 6 h induced samples. Induced samples for 12 h have approximately 2x more SAA than samples induced for 6 h, in both cytoplasmic and secreted quantification. Moreover, a statistical difference was observed between secreted-induced samples incubated for 6 h and 12 h. Similar results were reported in previous studies, where high levels of SAA were observed after cells were treated with IL-1B, IL-6, LPS, and Retinol [23,24]. LC/MS/MS analysis detected nine proteins (Table 1) interacting with SAA in samples induced for 12 hours. Notably, protein P23528 was detected in four samples, including two cytoplasmic controls and two induced cytoplasmic samples. Additionally, proteins with accession numbers Q14247, P30740, P13804, and P53396

were detected in three cytoplasmic samples, in two control and one induced sample or vice versa. The presence of protein P14555 was detected in two cytoplasmic controls and one supernatant control, suggesting that cytoplasmic components remained in the supernatant after separation. Proteins with accession numbers P07814 and Q02318 were only present in two cytoplasmic controls, suggesting that SAA may interact with these proteins, typically in hepatic cancer cells. In contrast, protein P05362 was only present in two cytoplasmic-induced samples, which might indicate that this protein interacts with SAA during inflammation and bacterial attacks. No results were obtained in samples incubated for 6 hours or in secreted samples induced for 12 hours.

Computational Predictions of Complexes' Physical Interactions

The ClusPro web server (http://nrc.bu.edu/cluster) from Boston University was used to simulate SAA protein complexes with the identified and characterized protein by LC/MS/MS. ClusPro was recognized as the best in the server category by the CAPRI (Critical Assessment of Predicted Interactions) and CASP (Critical Assessment of Protein Structure Prediction) convention [25]. After ClusPro docking, files were submitted to the PDBsum server, and the results were generated (Table 2). The results indicate that the Cofilin-1 complex has the lowest energy; meanwhile, the ATP-citrate synthase complex has the highest energy. Moreover, the Bifunctional glutamate/proline-tRNA ligase has a very strong interaction with SAA with 19 H-bonds and 4 salt bridges. In contrast, Sterol 26-hydroxylase, mitochondrial form, is the weakest complex with a single H-bond only. Interestingly, Cofilin-1 (CFL1), Phospholipase A2 (PLA2G2A), and Intercellular adhesion molecule 1 (ICAM1) are the top four protein complexes with the lowest energy and were found in the literature to have (at least) an indirect association with SAA. The results may support scientific data of SAA interacting with at least these three proteins since all these three predicted complexes have multiple H-bonds and at least one salt bridge, making these complexes relatively possible to be formed. A three-dimensional visualization of the physical interactions of predicted complexes can be observed in Figure 2.

Residues and domains that can be important in SAA interactions

Figure 3 shows seven of the most interacting residues of SAA involved in these complexes. The results revealed that Phe-11 and Trp-18 were present in all the predicted complexes, while Ile-65 and Leu 7 were present in eight and seven complexes, respectively. Phe-3, Arg-25, and Ile-58 were also present in six complexes. Notably, hydrophobic residues such as Phe and Ile were found to play a more significant role in these protein-protein interactions. Conversely, Arg-25, a polar/basic residue, was identified as being critical in forming salt bridges with the interacting proteins. Moreover, α-h1 and α-h2 were determined to be the helices that were most involved in complex interactions based on the results obtained. Furthermore, it was observed that most of these residues were hydrophobic and were part of the first 76 amino acid residues of SAA. These findings suggest that these residues play a crucial role in SAA interactions and contribute to their aggregation, a characteristic of Amyloidosis. A visual representation of the three-dimensional location of these residues is shown in Figure 3.

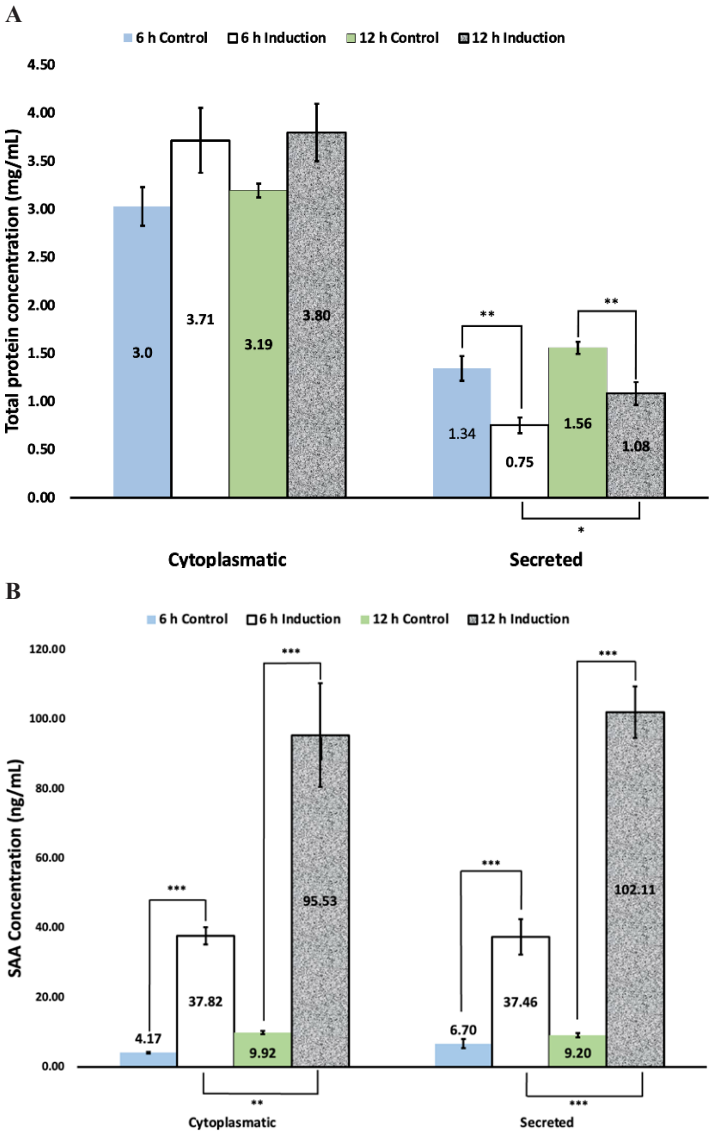

Figure 1: Total protein concentration was determined by QUBIT 3.0 (**A**) and SAA expression levels determined by ELISA (**B**). Cells were incubated in a serum-free medium for 6 h and 12 h, then treated with or without (negative controls) IL-1β, LPS, and Retinol. N = 3 (triplicates). Mean ± SEM is plotted. *p < 0.05; **p < 0.01; ***p < 0.001; p values were determined by a two-tailed t-test.

Table 1: Results of LC/MS/MS for samples incubated for 12 hours.

Protein		Samples**					
Accession	Description	1A	2A	3A	4A	5A	6A
P23528	Cofilin-1	X	X			X	X
P30740	Leukocyte elastase inhibitor	X				X	X
P14555	PhospholipasA2	X	X		X		
P05362	Intercellular adhesion molecule 1					X	X
Q14247	Src substrate cortactin	X	X			X	
P13804	Electron transfer flavoprotein subunit alpha	X	X				X
P07814	Bifunctional glutamate/proline--tRNA ligase	X	X				
Q02318	Sterol 26-hydroxylase	X	X				
P53396	ATP-citrate synthase	X	X				X

**1A and 2A are cytoplasmic samples without induction agents (controls); 3A and 4A are supernatant samples without induction agents (controls); 4A and 5A are cytoplasmic induced samples.

Table 2: Results for each protein-SAA interaction using the ClusPro web server.

Protein accession number	Energy	No. of H-bonds	No. of non-bonded contacts	No. of salt bridges	No. of interfaces residues	No. of interfaces residues for SAA
P23528	-795.4	5	130	3	20	14
P30740	-964.8	7	160	2	24	20
P14555	-1048	7	142	1	19	25
P05362	-1068	3	87	1	17	20
Q14247	-1122	13	139	4	24	28
P13804	-1163	12	155	2	21	20
P07814	-1203	19	163	4	25	23
Q02318	-1249	1	101	--	18	17
P53396	-1261	2	101	1	25	21

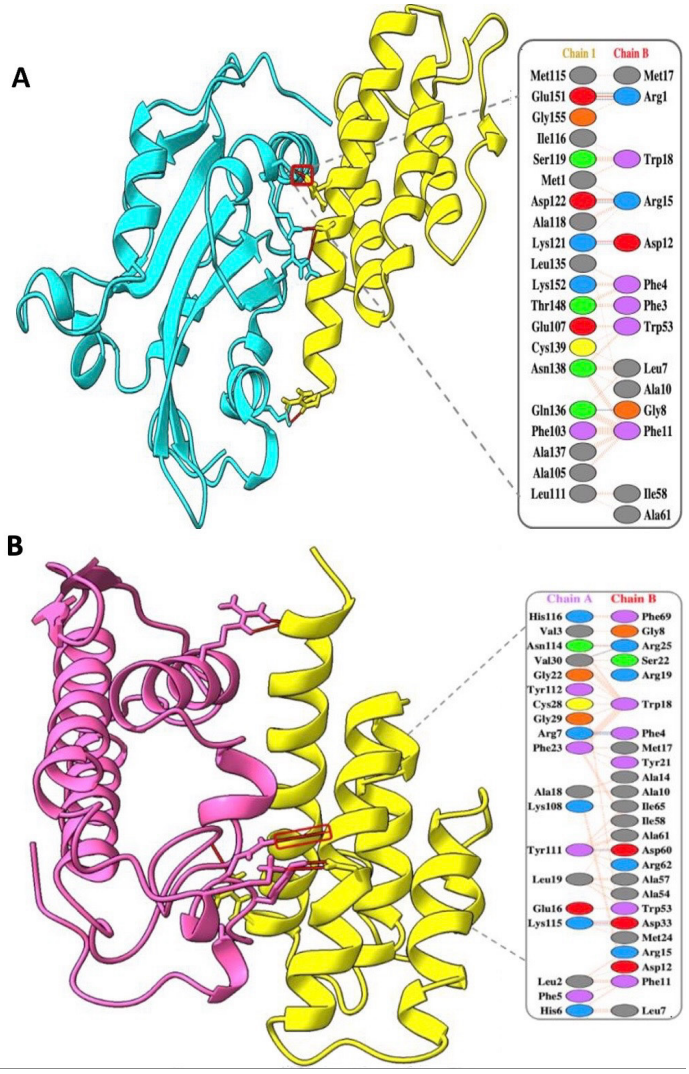

Figure 2: H-bonds (red) between SAA (yellow) and protein targets Cofilin-1(cyan, **A**), and Phospholipase A2 (pink, **B**). SAA complexes were generated with ClusPro and visualized with UCSF Chimera v1.2. Amino acid residues involved in these protein-protein interactions (PPIs) were described by PDBsum. These proteins were chosen explicitly for visualization since other publications associated them with SAA [26-28].

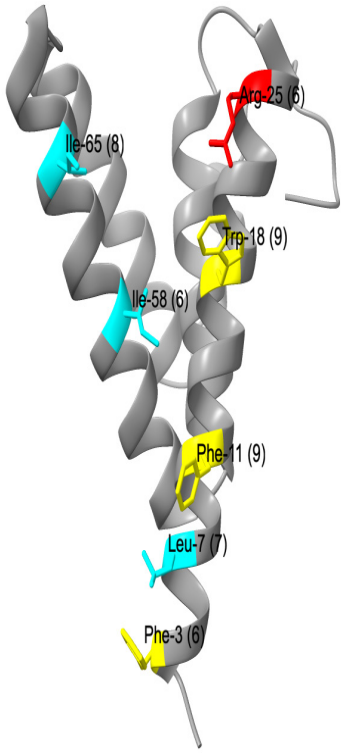

Figure 3: Three-dimensional representation of SAA. The most interactive residues in protein-protein complex simulations using ClusPro are as follows: cyan for hydrophobic residues, yellow for aromatic residues and red for polar/basic residues. The number of complexes where each residue interacts is in parenthesis. SAA was visualized with UCSF Chimera v1.2.

Possible new roles of SAA and support postulated ones

Nine proteins were characterized by LC-MS/MS that can possibly form complexes with SAA. However, only three of them were found to have at least an indirect association with SAA in the PubMed database. These three proteins were Cofilin-1 (CFL1), Phospholipase A2 (PLA2G2A), and Intercellular adhesion molecule 1 (ICAM1). CFL1 and SAA were associated with the wheal duration in Chronic spontaneous urticaria (CSU) patients and, therefore, could be considered new potential inflammatory biomarkers related to CSU [26]. Moreover, SAA solubilized lipid bilayers to generate substrates for sPLA2 and removed its bioactive products. Consequently, SAA and sPLA2 can act synergistically to remove cellular membrane debris from injured sites, a prerequisite for tissue healing [27]. Lastly, SAA perpetuates immune processes leading to joint damage and disability in RA synovium by functional up-regulation of ICAM-1 and promoting leukocyte adhesion, endothelial cells migration, and angiogenesis through the NF-kB pathway, which may provide novel targets for RA treatment [28].

According to LC/MS/MS, SAA might have new related functions or, at the very least, be able to explain some postulated or discovered ones. For instance, aggregates of Cofilin-1 were found to be associated with tau pathology and the onset of Alzheimer's disease [29], while SAA has been linked to Alzheimer's [30].

According to the results of the Cofilin-1 investigation, this protein denotes actions started early in the pathogenic cascade. With this knowledge, it is possible to hypothesize that SAA and Cofilin-1 may interact and contribute to the beta-amyloid aggregation in the brain that characterizes this harmful disease. As mentioned before, through its interaction with sPLA2, SAA promotes the removal of cellular membrane debris and tissue healing. However, by up-regulating ICAM-1 and promoting leukocyte adhesion, endothelial cell migration, and angiogenesis via the NF-kB pathway, SAA maintains immune processes that cause joint damage and disability in the RA synovium. Interestingly, Leukocyte elastase inhibitor protect cells from proteases released during stress or infection, inhibiting the activity of various neutrophil proteases and inflammatory caspases, and promoting beta-cell proliferation when secreted [31]. The interaction of SAA with these three proteins can have beneficial and harmful effects, suggesting that SAA has a role in the immune response.

As Cofilin-1, Src substrate cortactin (CTTN) plays multiple roles in the organization of the actin cytoskeleton and cell shape, regulating neuron morphology and spine density [32,33]. Moreover, CTTN promotes cancer cell invasiveness and metastasis [34]. SAA interacting with these two proteins suggested a possible role of this serum protein in actin regulation, neuronal morphogenesis, and morphology. Moreover, part of the SAA elevated levels in the bloodstream can be due to its interaction with CTTN in promoting cancer cell invasiveness and metastasis.

Electron transfer flavoprotein subunit alpha (ETFA) accepts electrons from mitochondrial dehydrogenases and transfers them to the main mitochondrial respiratory chain, required for normal mitochondrial fatty acid oxidation [35]. Moreover, ATP-citrate synthase catalyzes citrate cleavage into oxaloacetate and acetyl-CoA, a common substrate for de novo cholesterol and fatty acid synthesis [36]. In contrast, Bifunctional glutamate/proline--tRNA ligase helps bring in and store fatty acids in the cells [37]. At the same time, Sterol 26-hydroxylase regulates cholesterol homeostasis [38]. SAA interacting with these four proteins suggested the role of SAA in cholesterol regulation, as mentioned in published research. Table 3 summarizes all the detected proteins and their related functions.

Table 3: Accession number and functions of each detected protein by LC/MS/MS.

Accession number	Primary function	Reference
P23528	Binding actin protein and Neural tube morphogenesis and neural crest cell migration.	[32]
P30740	A neutrophil serine protease inhibitor plays a vital role in regulating the innate immune response, inflammation, and cellular homeostasis by protecting cells from proteases released during stress or infection.	[31]
P14555	A secretory calcium-dependent phospholipase A2 targets extracellular phospholipids and contributes to host antimicrobial defense, lipid remodeling of cellular membranes, and tissue regeneration.	[27]
P05362	Act as ligands for leukocyte adhesion protein LFA-1 during leukocyte trans- endothelial migration, promoting the assembly of endothelial apical cups.	[39]
Q14247	Contribute to the organization of the actin cytoskeleton and cell shape, regulating neuron morphology and spine density, playing a role in focal adhesion assembly and turnover, regulating cortical actin-based cytoskeletal rearrangement, intracellular protein transport, and promoting cancer cell invasiveness and metastasis.	[33,34]
P13804	Accepts electrons from mitochondrial dehydrogenases and transfers them to the main mitochondrial respiratory chain, required for normal mitochondrial fatty acid oxidation and amino acid metabolism.	[35]
P07814	Promote the uptake of long-chain fatty acid by adipocytes and indirectly influences lifespan.	[37]
Q02318	Catalyzes the regio- and stereospecific hydroxylation of cholesterol, its derivatives and regulates cholesterol homeostasis.	[38]
P53396	Catalyzes the cleavage of citrate into oxaloacetate and acetyl-CoA, the latter serving as common substrate for de novo cholesterol and fatty acid synthesis.	[36]

Conclusion

SAA overexpression and SAA-antibody coupling was supported via Western blot before Co-Immunoprecipitation. Isolated SAA-protein complexes were characterized using liquid chromatography-tandem mass spectrometry (LC/MS/MS), where nine proteins were identified. The interactions of SAA with PLA2, ICAM-1, and Leukocyte elastase inhibitor suggest that SAA has a role in the immune response. Meanwhile, SAA interacting with Cofilin-1 and Src substrate cortactin (CTTN) suggests a possible role of this serum protein in actin regulation, neuronal morphogenesis, and morphology. Moreover, part of the SAA elevated levels in the bloodstream can be due to its interaction with CTTN in promoting cancer cell invasiveness and metastasis. Interestingly, SAA interacting with Electron transfer flavoprotein subunit alpha, ATP-citrate synthase, and Bifunctional glutamate/proline-tRNA ligase suggested the role of SAA in cholesterol regulation.

As highlighted, only CFL1, PLA2G2A and ICAM1 were found to have at least an indirect association with SAA in scientific publications. CFL1 and SAA were associated with the wheal duration in Chronic spontaneous urticaria (CSU) patients. In contrast, SAA and PLA2 may act synergistically to remove cellular membrane debris from injured sites, a prerequisite for tissue healing. Lastly, SAA perpetuates immune processes leading to joint damage and disability in RA synovium by functional up-regulation of ICAM-1 and promoting leukocyte adhesion, endothelial cell migration, and angiogenesis. Moreover, the investigation into Cofilin-1 suggests that it denotes early actions in the pathogenic cascade of tau pathology. Thus, it is possible that SAA and Cofilin-1 could interact and contribute to the development of Alzheimer's disease.

The study findings suggested the involvement of serum amyloid A (SAA) in immune response and cholesterol regulation. Furthermore, the results suggested a novel role of SAA in regulating actin and promoting neuronal morphogenesis. Interestingly, as previous research stipulated, these findings supported the hypothesis that SAA may have a role in Alzheimer, Cancer, and Rheumatoid arthritis. Overall, the results of this research support some already

established roles of SAA and provide new information related to its protein-protein interactions that could be used to develop new therapeutic interventions and diagnostic tools for diseases associated with SAA.

Acknowledgements

This research was supported by the Puerto Rico IDeA Network of Biomedical Research Excellence, an Institutional Development Award (IDeA) from the National Institute of General Medical Sciences of the National Institutes of Health under grant no. P20GM103475. Thanks to Ana Rodríguez and Yadira M. Cantres, lab technicians, and Dr. Loyda M. Meléndez, Translational Proteomics Center Core Director of the Comprehensive Cancer Center UPR at San Juan, Puerto Rico, for providing technical help in this project. Research infrastructure support and services were provided, in part, by the grant U54MD007600 from the National Institute on Minority Health and Health Disparities (NIMHD). The INBRE program NIH-NCRR-P20-RR016473 at the University of Puerto Rico-Medical Sciences Campus also supports this facility.

References

1. Yoo JY, Desiderio S. Innate and acquired immunity intersect in a global view of the acute-phase response. Proc Natl Acad Sci U S A. 2003; 100: 1157-1162.
2. Urieli-Shoval S, Cohen P, Eisenberg S, et al. Widespread expression of serum amyloida A in histologically normal human tissues: Predominant localization to the epithelium. J Histochem Cytochem. 1998; 46: 1377-1384.
3. Sack GH, Zachara N, Rosenblum N, et al. Serum amyloid A1 (SAA1) protein in human colostrum. FEBS Open Bio. 2018; 8: 435-441.
4. Sack JR GH, MCZ. Synovial Cells During Retroviral Arthritis. 1992; 141: 525-529.
5. Tucker PC, Sack JR GH. Expression of serum amyloid A genes in mouse brain: unprecedented response to inflammatory mediators. FASEB J. 2001; 15: 2241-2246.
6. Larson MA, Wei SH, Weber A, et al. Induction of human mammary-associated serum amyloid A3 expression by prolactin or lipopolysaccharide. Biochem Biophys Res Commun. 2003; 301: 1030-1037.
7. Ganal SC, MacPherson AJ. An ambulance for retinol. Elife. 2014; 3: 04246.
8. Gillmore JD, Lovat LB, Persey MR, et al. Amyloid load and clinical outcome in AA amyloidosis in relation to circulating concentration of serum amyloid A protein. Lancet. 2001; 358: 24-29.
9. Agilli M, Aydin FN, Cayci T, et al. Evaluation of Serum Amyloid A as a Marker of Persistent Inflammation in Patients with Rheumatoid Arthritis. Mediators Inflamm. 2015; 2015: 843152.
10. Röcken C, Shakespeare A. Pathology, diagnosis and pathogenesis of AA amyloidosis. Virchows Archiv. 2002; 440: 111-122.
11. Van der Hilst JCH, Yamada T, Op den Camp HJM, et al. Increased susceptibility of serum amyloid A 1.1 to degradation by MMP-1: potential explanation for higher risk of type AA amyloidosis. Rheumatology (Oxford). 2008; 47: 1651-1654.
12. Röcken C, Menard R, Bühling F, et al. Proteolysis of serum amyloid A and AA amyloid proteins by cysteine proteases: Cathepsin B generates AA amyloid proteins and cathepsin L may prevent their formation. Ann Rheum Dis. 2005; 64: 808-815.
13. Siegmund SV, Schlosser M, Schildberg FA, et al. Serum amyloid a induces inflammation, proliferation and cell death in activated hepatic stellate cells. PLoS One. 2016; 11: 0150893.
14. Malle E, De Beer FC. Human serum amyloid A (SAA) protein: A prominent acute-phase reactant for clinical practice. Eur J Clin Invest. 1996; 26: 427-435.
15. Zinellu A, Paliogiannis P, Carru C, et al. Serum amyloid A concentrations, COVID-19 severity and mortality: An updated systematic review and meta-analysis. Int J Infect Dis. 2021; 105: 668-674.
16. María Teresa Donato, María José Gómez-Lechón LT. Culture and Functional Characterization of Human Hepatoma HepG2 Cells. Protocols in In Vitro Hepatocyte Research. 2015; 1250: 77-93.
17. Gattu S, Bang YJ, Pendse M, et al. Epithelial retinoic acid receptor β regulates serum amyloid A expression and Vitamin A-dependent intestinal immunity. Proc Natl Acad Sci U S A. 2019; 166: 10911-10916.
18. Jumeau C, Awad F, Assrawi E, et al. Expression of SAA1, SAA2 and SAA4 genes in human primary monocytes and monocyte-derived macrophages. PLoS One. 2019; 14: 0217005.
19. https://docs.lib.purdue.edu/dissertations/AAI3033145
20. Caillet J, Baron B, Boni IV, et al. Identification of protein-protein and ribonucleoprotein complexes containing Hfq. Scientific Reports. 2019; 9: 1-12.
21. Wang X, Li W, Lu J, et al. Lipopolysaccharide suppresses albumin expression by activating NF-KappaB in rat hepatocytes. J Surg Res. 2004; 122: 274-279.
22. Zoico E, Roubenoff R. The role of cytokines in regulating protein metabolism and muscle function. Nutr Rev. 2002; 60: 39-51.
23. Derebe MG, Zlatkov CM, Gattu S, et al. Serum amyloid A is a retinol binding protein that transports retinol during bacterial infection. Elife. 2014; 3: 1-18.
24. Migita K, Abiru S, Nakamura M, et al. Lipopolysaccharide signaling induces serum amyloid A (SAA) synthesis in human hepatocytes in vitro. FEBS Lett. 2004; 569: 235-239.
25. Desta IT, Porter KA, Xia B, et al. Performance and its limits in rigid body protein-protein docking. Structure. 2020; 28: 1071.
26. Cao Y, Xu S, Kong W, et al. Identification and validation of differentially expressed proteins in serum of CSU patients with different duration of wheals using an iTRAQ labeling, 2D-LC-MS/MS. Exp Ther Med. 2018; 16: 4527.

27. Jayaraman S, Fändrich M, Gursky O. Synergy between serum amyloid A and secretory phospholipase A2. Elife. 2019; 8: 46630.

28. Mullan RH, Bresnihan B, Golden-Mason L, et al. Acute-phase serum amyloid A stimulation of angiogenesis, leukocyte recruitment, and matrix degradation in rheumatoid arthritis through an NF-κB-dependent signal transduction pathway. Arthritis Rheum. 2006; 54: 105-114.

29. Rahman T, Davies DS, Tannenberg RK, et al. Cofilin Rods and Aggregates Concur with Tau Pathology and the Development of Alzheimer's Disease. J Alzheimers Dis. 2014; 42: 1443-1460.

30. Chung TF, Sipe JD, McKee A, et al. Serum amyloid A in Alzheimer's disease brain is predominantly localized to myelin sheaths and axonal membrane. Amyloid. 2000; 7: 105-110.

31. Cooley J, Takayama TK, Shapiro SD, et al. The serpin MNEI inhibits elastase-like and chymotrypsin-like serine proteases through efficient reactions at two active sites. Biochemistry. 2001; 40: 15762-15770.

32. Von Holleben M, Gohla A, Janssen KP, et al. Immunoinhibitory adapter protein Src homology domain 3 lymphocyte protein 2 (SLy2) regulates actin dynamics and B cell spreading. J Biol Chem. 2011; 286: 13489-13501.

33. Dudek SM, Chiang ET, Camp SM, et al. Abl tyrosine kinase phosphorylates nonmuscle Myosin light chain kinase to regulate endothelial barrier function. Mol Biol Cell. 2010; 21: 4042-4056.

34. Hashimoto S, Hirose M, Hashimoto A, et al. Targeting AMAP1 and cortactin binding bearing an atypical src homology 3/ proline interface for prevention of breast cancer invasion and metastasis. Proc Natl Acad Sci U S A. 2006; 103: 7036.

35. Freneaux E, Sheffield VC, Molin L, et al. Glutaric acidemia type II. Heterogeneity in beta-oxidation flux, polypeptide synthesis, and complementary DNA mutations in the alpha subunit of electron transfer flavoprotein in eight patients. J Clin Invest. 1992; 90: 1679-1686.

36. Lin R, Tao R, Gao X, et al. Acetylation stabilizes ATP-citrate lyase to promote lipid biosynthesis and tumor growth. Mol Cell. 2013; 51: 506-518.

37. Arif A, Terenzi F, Potdar AA, et al. EPRS is a critical mTORC1-S6K1 effector that influences adiposity in mice. Nature. 2017; 542: 357-361.

38. Pikuleva IA, Babiker A, Waterman MR, et al. Activities of recombinant human cytochrome P450c27 (CYP27) which produce intermediates of alternative bile acid biosynthetic pathways. J Biol Chem. 1998; 273: 18153-18160.

39. Van Buul JD, Allingham MJ, Samson T, et al. RhoG regulates endothelial apical cup assembly downstream from ICAM1 engagement and is involved in leukocyte trans-endothelial migration. J Cell Biol. 2007; 178: 1279.